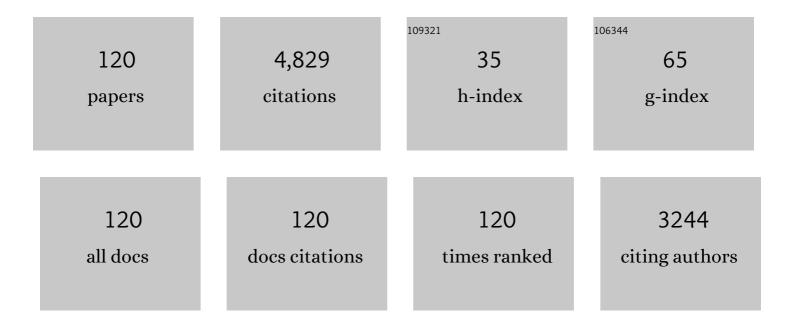
List of Publications by Year in descending order

Source: https://exaly.com/author-pdf/3332466/publications.pdf Version: 2024-02-01



#	Article	IF	CITATIONS
1	The M+1AX phases: Materials science and thin-film processing. Thin Solid Films, 2010, 518, 1851-1878.	1.8	934
2	Mn+1AXnphases in theTiâ^'Siâ^'Csystem studied by thin-film synthesis andab initiocalculations. Physical Review B, 2004, 70, .	3.2	212
3	Deposition and characterization of ternary thin films within the Ti–Al–C system by DC magnetron sputtering. Journal of Crystal Growth, 2006, 291, 290-300.	1.5	212
4	Thermal stability of Ti3SiC2 thin films. Acta Materialia, 2007, 55, 1479-1488.	7.9	198
5	Growth and characterization of MAX-phase thin films. Surface and Coatings Technology, 2005, 193, 6-10.	4.8	176
6	Growth of Ti3SiC2 thin films by elemental target magnetron sputtering. Journal of Applied Physics, 2004, 96, 4817-4826.	2.5	158
7	Epitaxial Ti2GeC, Ti3GeC2, and Ti4GeC3 MAX-phase thin films grown by magnetron sputtering. Journal of Materials Research, 2005, 20, 779-782.	2.6	125
8	High-power impulse magnetron sputtering of Ti–Si–C thin films from a Ti3SiC2 compound target. Thin Solid Films, 2006, 515, 1731-1736.	1.8	96
9	Ti2AlC coatings deposited by High Velocity Oxy-Fuel spraying. Surface and Coatings Technology, 2008, 202, 5976-5981.	4.8	84
10	Tribofilm formation on cemented carbides in dry sliding conformal contact. Wear, 2000, 239, 219-228.	3.1	80
11	Sputter deposition from a Ti2AlC target: Process characterization and conditions for growth of Ti2AlC. Thin Solid Films, 2010, 518, 1621-1626.	1.8	77
12	Theory of the effects of substitutions on the phase stabilities of Ti1â ^{~,} xAlxN. Journal of Applied Physics, 2003, 93, 4505-4511.	2.5	75
13	Ta4AlC3: Phase determination, polymorphism and deformation. Acta Materialia, 2007, 55, 4723-4729.	7.9	75
14	Structural, electrical, and mechanical properties of nc-TiCâ^•a-SiC nanocomposite thin films. Journal of Vacuum Science & Technology an Official Journal of the American Vacuum Society B, Microelectronics Processing and Phenomena, 2005, 23, 2486.	1.6	69
15	Growth of High Quality Epitaxial Rhombohedral Boron Nitride. Crystal Growth and Design, 2012, 12, 3215-3220.	3.0	60
16	Electronic structure investigation ofTi3AlC2,Ti3SiC2, andTi3GeC2by soft x-ray emission spectroscopy. Physical Review B, 2005, 72, .	3.2	59
17	Magnetron sputtering of Ti3SiC2 thin films from a compound target. Journal of Vacuum Science and Technology A: Vacuum, Surfaces and Films, 2007, 25, 1381-1388.	2.1	58
18	Growth of Ti-C nanocomposite films by reactive high power impulse magnetron sputtering under industrial conditions. Surface and Coatings Technology, 2012, 206, 2396-2402.	4.8	58

#	Article	IF	CITATIONS
19	ZrB2 thin films grown by high power impulse magnetron sputtering from a compound target. Thin Solid Films, 2012, 526, 163-167.	1.8	58
20	Structural, electrical and mechanical characterization of magnetron-sputtered V–Ge–C thin films. Acta Materialia, 2008, 56, 2563-2569.	7.9	55
21	Low resistivity ohmic titanium carbide contacts to n- and p-type 4H-silicon carbide. Solid-State Electronics, 2000, 44, 1179-1186.	1.4	48
22	Review of transition-metal diboride thin films. Vacuum, 2022, 196, 110567.	3.5	48
23	Nanocomposite Al2O3–ZrO2 thin films grown by reactive dual radio-frequency magnetron sputtering. Thin Solid Films, 2008, 516, 4977-4982.	1.8	47
24	Hard and elastic epitaxial ZrB2 thin films on Al2O3(0001) substrates deposited by magnetron sputtering from a ZrB2 compound target. Acta Materialia, 2016, 111, 166-172.	7.9	47
25	First-principles calculations on the structural evolution of solid fullerene-like CPx. Chemical Physics Letters, 2006, 426, 374-379.	2.6	46
26	Epitaxial CVD growth of sp ² â€hybridized boron nitride using aluminum nitride as buffer layer. Physica Status Solidi - Rapid Research Letters, 2011, 5, 397-399.	2.4	44
27	A theoretical investigation of mixing thermodynamics, age-hardening potential and electronic structure of ternary M11–xM2xB2 alloys with AlB2 type structure. Scientific Reports, 2015, 5, 9888.	3.3	44
28	Phase transformation in \hat{I}^{a} - and \hat{I}^{3} -Al2O3 coatings on cutting tool inserts. Surface and Coatings Technology, 2009, 203, 1682-1688.	4.8	43
29	High-rate deposition of amorphous and nanocomposite Ti–Si–C multifunctional coatings. Surface and Coatings Technology, 2010, 205, 299-305.	4.8	42
30	Strategy for simultaneously increasing both hardness and toughness in ZrB2-rich Zr1â^'xTaxBy thin films. Journal of Vacuum Science and Technology A: Vacuum, Surfaces and Films, 2019, 37, .	2.1	42
31	Fullerene-like CPx: A first-principles study of the relative stability of precursors and defect energetics during synthetic growth. Thin Solid Films, 2006, 515, 1028-1032.	1.8	40
32	Homoepitaxial growth of Ti–Si–C MAX-phase thin films on bulk Ti3SiC2 substrates. Journal of Crystal Growth, 2007, 304, 264-269.	1.5	40
33	Synthesis of phosphorusâ€carbide thin films by magnetron sputtering. Physica Status Solidi - Rapid Research Letters, 2008, 2, 191-193.	2.4	40
34	Microstructure of high velocity oxy-fuel sprayed Ti2AlC coatings. Journal of Materials Science, 2010, 45, 2760-2769.	3.7	40
35	Photoemission studies ofTi3SiC2and nanocrystalline-TiC/amorphous-SiC nanocomposite thin films. Physical Review B, 2006, 74, .	3.2	37
36	Direct current magnetron sputtered ZrB2 thin films on 4H-SiC(0001) and Si(100). Thin Solid Films, 2014, 550, 285-290.	1.8	35

#	Article	IF	CITATIONS
37	Micro and macroscale tribological behavior of epitaxial Ti3SiC2 thin films. Wear, 2008, 264, 914-919.	3.1	34
38	Weak electronic anisotropy in the layered nanolaminate Ti 2 GeC. Solid State Communications, 2008, 146, 498-501.	1.9	33
39	Stoichiometric, epitaxial ZrB2 thin films with low oxygen-content deposited by magnetron sputtering from a compound target: Effects of deposition temperature and sputtering power. Journal of Crystal Growth, 2015, 430, 55-62.	1.5	33
40	Electrical characterization of TiC ohmic contacts to aluminum ion implanted 4H–silicon carbide. Applied Physics Letters, 2000, 77, 1478-1480.	3.3	32
41	Chemical vapour deposition of epitaxial rhombohedral BN thin films on SiC substrates. CrystEngComm, 2014, 16, 5430-5436.	2.6	32
42	Review Article: Challenge in determining the crystal structure of epitaxial 0001 oriented sp2-BN films. Journal of Vacuum Science and Technology A: Vacuum, Surfaces and Films, 2018, 36, .	2.1	32
43	Boron nitride: A new photonic material. Physica B: Condensed Matter, 2014, 439, 29-34.	2.7	31
44	Microstructure evolution of Ti–Si–C–Ag nanocomposite coatings deposited by DC magnetron sputtering. Acta Materialia, 2010, 58, 6592-6599.	7.9	30
45	Anisotropy in the electronic structure of <mml:math xmlns:mml="http://www.w3.org/1998/Math/MathML" display="inline"> <mml:mrow> <mml:msub> <mml:mtext> V </mml:mtext> <mml:mn>2 </mml:mn> </mml:msub> <r by soft x-ray emission spectroscopy and first-principles theory. Physical Review B. 2008, 78</r </mml:mrow></mml:math 	nm <mark>8:12</mark> text	⊳Ge [®]
46	SiN _{<i>x</i>} Coatings Deposited by Reactive High Power Impulse Magnetron Sputtering: Process Parameters Influencing the Nitrogen Content. ACS Applied Materials & amp; Interfaces, 2016, 8, 20385-20395.	8.0	28
47	Polytype Pure sp ² -BN Thin Films As Dictated by the Substrate Crystal Structure. Chemistry of Materials, 2015, 27, 1640-1645.	6.7	26
48	High-temperature nanoindentation of epitaxial ZrB2 thin films. Scripta Materialia, 2016, 124, 117-120.	5.2	25
49	Deposition of Transition Metal Carbides and Superlattices Using C[sub 60] as Carbon Source. Journal of the Electrochemical Society, 2000, 147, 3361.	2.9	24
50	Microstructure and electrical properties of Ti–Si–C–Ag nanocomposite thin films. Surface and Coatings Technology, 2007, 201, 6465-6469.	4.8	23
51	Direct current magnetron sputtering deposition of nanocomposite alumina — zirconia thin films. Thin Solid Films, 2008, 516, 8352-8358.	1.8	23
52	On the effect of silicon in CVD of sp2hybridized boron nitride thin films. CrystEngComm, 2013, 15, 455-458.	2.6	23
53	Chemical vapour deposition of tungsten carbides on tantalum and nickel substrates. Thin Solid Films, 1996, 272, 116-123.	1.8	22
54	Growth and Property Characterization of Epitaxial MAX-Phase Thin Films from the Ti _{n+1} (Si, Ge, Sn)C _n Systems. Advances in Science and Technology, 2006, 45, 2648.	0.2	22

#	Article	IF	CITATIONS
55	Electrical resistivity of Ti <i>_n</i> ₊₁ AC <i>_n</i> (A = Si, Ge, Sn, <i>n) Tj E</i>	IQq1_1 0.: 2.6	784314 rgBT
56	Magnetron sputtering of epitaxial Zr <scp>B</scp> ₂ thin films on 4 <scp>H</scp> â€ <scp>S</scp> i <scp>C</scp> (0001) and Si(111). Physica Status Solidi (A) Applications and Materials Science, 2014, 211, 636-640.	1.8	22
57	SiNx coatings deposited by reactive high power impulse magnetron sputtering: Process parameters influencing the residual coating stress. Journal of Applied Physics, 2017, 121, .	2.5	20
58	Chemical bonding in epitaxial ZrB2 studied by X-ray spectroscopy. Thin Solid Films, 2018, 649, 89-96.	1.8	20
59	Electronic structure of β-Ta films from X-ray photoelectron spectroscopy and first-principles calculations. Applied Surface Science, 2019, 470, 607-612.	6.1	20
60	Low temperature epitaxial growth of metal carbides using fullerenes. Surface and Coatings Technology, 2001, 142-144, 817-822.	4.8	19
61	Epitaxial TiC/SiC multilayers. Physica Status Solidi - Rapid Research Letters, 2007, 1, 113-115.	2.4	19
62	Experiments and modeling of dual reactive magnetron sputtering using two reactive gases. Journal of Vacuum Science and Technology A: Vacuum, Surfaces and Films, 2008, 26, 565-570.	2.1	19
63	Atomic Layer Deposition of Ta2O5 Using the TaI5 and O2 Precursor Combination. Chemical Vapor Deposition, 2003, 9, 245-248.	1.3	18
64	Silicon oxynitride films deposited by reactive high power impulse magnetron sputtering using nitrous oxide as a single-source precursor. Journal of Vacuum Science and Technology A: Vacuum, Surfaces and Films, 2015, 33, .	2.1	18
65	Magnetron Sputter Epitaxy of High-Quality GaN Nanorods on Functional and Cost-Effective Templates/Substrates. Energies, 2017, 10, 1322.	3.1	18
66	Deposition and characterisation of NbxC60 films. Thin Solid Films, 2002, 405, 42-49.	1.8	17
67	Structure and properties of phosphorus-carbide thin solid films. Thin Solid Films, 2013, 548, 247-254.	1.8	17
68	Initial stages of growth and the influence of temperature during chemical vapor deposition of sp2-BN films. Journal of Vacuum Science and Technology A: Vacuum, Surfaces and Films, 2015, 33, .	2.1	17
69	Cryogenic deposition of carbon nitride thin solid films by reactive magnetron sputtering; suppression of the chemical desorption processes. Thin Solid Films, 2005, 478, 34-41.	1.8	16
70	Bonding Structures of ZrH _{<i>x</i>} Thin Films by X-ray Spectroscopy. Journal of Physical Chemistry C, 2017, 121, 25750-25758.	3.1	16
71	Gas Phase Chemistry of Trimethylboron in Thermal Chemical Vapor Deposition. Journal of Physical Chemistry C, 2017, 121, 26465-26471.	3.1	16
72	Conductive nanocomposite ceramics as tribological and electrical contact materials. EPJ Applied Physics, 2010, 49, 22902.	0.7	15

#	Article	IF	CITATIONS
73	Influence of Substrate Heating and Nitrogen Flow on the Composition, Morphological and Mechanical Properties of SiNx Coatings Aimed for Joint Replacements. Materials, 2017, 10, 173.	2.9	15
74	Growth, structure, and mechanical properties of transition metal carbide superlattices. Journal of Materials Research, 2001, 16, 1301-1310.	2.6	14
75	Theoretical and experimental study of metastable solid solutions and phase stability within the immiscible Ag-Mo binary system. Journal of Applied Physics, 2016, 119, .	2.5	14
76	Silicon carbonitride thin films deposited by reactive high power impulse magnetron sputtering. Surface and Coatings Technology, 2018, 335, 248-256.	4.8	14
77	Surface-Inhibiting Effect in Chemical Vapor Deposition of Boron–Carbon Thin Films from Trimethylboron. Chemistry of Materials, 2019, 31, 5408-5412.	6.7	14
78	Towards Functional Silicon Nitride Coatings for Joint Replacements. Coatings, 2019, 9, 73.	2.6	14
79	Deposition of epitaxial transition metal carbide films and superlattices by simultaneous direct current metal magnetron sputtering and C ₆₀ evaporation. Journal of Materials Research, 2001, 16, 633-643.	2.6	13
80	Intrusion-type deformation in epitaxial Ti3SiC2â^•TiC0.67 nanolaminates. Applied Physics Letters, 2007, 91, .	3.3	13
81	Reactive sputtering of CSx thin solid films using CS2 as precursor. Vacuum, 2020, 182, 109775.	3.5	13
82	In situmonitoring of size distributions and characterization of nanoparticles during W ablation in N2 atmosphere. Journal of Applied Physics, 2003, 94, 2011-2017.	2.5	12
83	On the effect of water and oxygen in chemical vapor deposition of boron nitride. Thin Solid Films, 2012, 520, 5889-5893.	1.8	12
84	Plasma CVD of B–C–N thin films using triethylboron in argon–nitrogen plasma. Journal of Materials Chemistry C, 2020, 8, 4112-4123.	5.5	12
85	Comment on ?Pulsed Laser Deposition and Properties of M n+1AX x Phase Formulated Ti3SiC2 Thin Films?. Tribology Letters, 2004, 17, 977-978.	2.6	11
86	Thermal chemical vapor deposition of epitaxial rhombohedral boron nitride from trimethylboron and ammonia. Journal of Vacuum Science and Technology A: Vacuum, Surfaces and Films, 2019, 37, .	2.1	11
87	β-Ta and α-Cr thin films deposited by high power impulse magnetron sputtering and direct current magnetron sputtering in hydrogen containing plasmas. Physica B: Condensed Matter, 2014, 439, 3-8.	2.7	10
88	A simple model for non-saturated reactive sputtering processes. Thin Solid Films, 2019, 688, 137413.	1.8	10
89	Atom probe tomography field evaporation characteristics and compositional corrections of ZrB2. Materials Characterization, 2019, 156, 109871.	4.4	10
90	The Effect of N, C, Cr, and Nb Content on Silicon Nitride Coatings for Joint Applications. Materials, 2020, 13, 1896.	2.9	10

#	Article	IF	CITATIONS
91	ZrB2 thin films deposited on GaN(0001) by magnetron sputtering from a ZrB2 target. Journal of Crystal Growth, 2016, 453, 71-76.	1.5	9
92	Synthesis and properties of CS _{<i>x</i>} F _{<i>y</i>} thin films deposited by reactive magnetron sputtering in an Ar/SF ₆ discharge. Journal of Physics Condensed Matter, 2017, 29, 195701.	1.8	9
93	Electronic properties and bonding in <mml:math xmlns:mml="http://www.w3.org/1998/Math/MathML"><mml:mrow><mml:mi>Zr</mml:mi><mml:msub><mml:mi mathvariant="normal">H<mml:mi></mml:mi></mml:mi </mml:msub></mml:mrow> thin films investigated by valence-band x-ray photoelectron spectroscopy. Physical Review B. 2017. 96.</mml:math 	3.2	9
94	Cubic boron phosphide epitaxy on zirconium diboride. Journal of Crystal Growth, 2018, 483, 115-120.	1.5	9
95	Rhombohedral and turbostratic boron nitride: X-ray diffraction and photoluminescence signatures. Applied Physics Letters, 2021, 119, .	3.3	9
96	The influence of the deposition angle on the composition of reactively sputtered thin films. Surface and Coatings Technology, 1997, 94-95, 242-246.	4.8	8
97	Early stages of growth and crystal structure evolution of boron nitride thin films. Japanese Journal of Applied Physics, 2016, 55, 05FD06.	1.5	8
98	The Effect of Coating Density on Functional Properties of SiNx Coated Implants. Materials, 2019, 12, 3370.	2.9	8
99	Compositional dependence of epitaxial Tin+1SiCn MAX-phase thin films grown from a Ti3SiC2 compound target. Journal of Vacuum Science and Technology A: Vacuum, Surfaces and Films, 2019, 37, .	2.1	8
100	Ti thin films deposited by high-power impulse magnetron sputtering in an industrial system: Process parameters for a low surface roughness. Vacuum, 2022, 195, 110698.	3.5	8
101	Deposition of transition metal carbide superlattices using C60 as a carbon source. Applied Physics Letters, 1998, 73, 2754-2756.	3.3	7
102	Strain relaxation of low-temperature deposited epitaxial titanium-carbide films. Journal of Crystal Growth, 2000, 219, 237-244.	1.5	7
103	In Situ Control of the Oxide Layer on Thermally Evaporated Titanium and Lysozyme Adsorption by Means of Electrochemical Quartz Crystal Microbalance with Dissipation. ACS Applied Materials & Interfaces, 2009, 1, 301-310.	8.0	7
104	Ni and Ti diffusion barrier layers between Ti–Si–C and Ti–Si–C–Ag nanocomposite coatings and Cu-based substrates. Surface and Coatings Technology, 2012, 206, 2558-2565.	4.8	7
105	Reactive sputtering of δ-ZrH2 thin films by high power impulse magnetron sputtering and direct current magnetron sputtering. Journal of Vacuum Science and Technology A: Vacuum, Surfaces and Films, 2014, 32, .	2.1	7
106	Thermodynamic stability of hexagonal and rhombohedral boron nitride under chemical vapor deposition conditions from van der Waals corrected first principles calculations. Journal of Vacuum Science and Technology A: Vacuum, Surfaces and Films, 2019, 37, .	2.1	7
107	Rhombohedral boron nitride epitaxy on ZrB2. Journal of Vacuum Science and Technology A: Vacuum, Surfaces and Films, 2021, 39, .	2.1	7
108	Bonding mechanism in the transition-metal fullerides studied by symmetry-selective resonant x-ray inelastic scattering. Physical Review B, 2001, 63, .	3.2	6

#	Article	IF	CITATIONS
109	Theoretical Prediction and Synthesis of CS _{<i>x</i>} F _{<i>y</i>} Thin Films. Journal of Physical Chemistry C, 2016, 120, 9527-9534.	3.1	6
110	Reactive magnetron sputtering of tungsten target in krypton/trimethylboron atmosphere. Thin Solid Films, 2019, 688, 137384.	1.8	6
111	Arrhenius-type temperature dependence of the chemical desorption processes active during deposition of fullerene-like carbon nitride thin films. Surface Science, 2004, 569, L289-L295.	1.9	5
112	Phase identification in γ- and κ-alumina coatings by cathodoluminescence. Scripta Materialia, 2009, 61, 379-382.	5.2	3
113	Effect of low-energy ion assistance on the properties of sputtered ZrB2 films. Vacuum, 2022, 195, 110688.	3.5	3
114	Chemical vapor deposition of sp2-boron nitride films on Al2O3 (0001), (112Â ⁻), (11Â ⁻ 02), and (101Â ⁻) substrates. Journal of Vacuum Science and Technology A: Vacuum, Surfaces and Films, 2022, 40, .	2.1	3
115	Structural and Mechanical Properties of CN _X and CP _{X } Thin Solid Films. Key Engineering Materials, 0, 488-489, 581-584.	0.4	2
116	Contact Resistance of Ti-Si-C-Ag and Ti-Si-C-Ag-Pd Nanocomposite Coatings. Journal of Electronic Materials, 2012, 41, 560-567.	2.2	2
117	Stoichiometric silicon oxynitride thin films reactively sputtered in Ar/N2O plasmas by HiPIMS. Journal Physics D: Applied Physics, 2016, 49, 135309.	2.8	2
118	Synthesis and characterization of Ti-Si-C compounds for electrical contact applications. , 0, , .		1
119	Chemical vapor deposition of sp2-boron nitride on Si(111) substrates from triethylboron and ammonia: Effect of surface treatments. Journal of Vacuum Science and Technology A: Vacuum, Surfaces and Films, 2020, 38, .	2.1	1
120	Elucidating Pathfinding Elements from the Kubi Gold Mine in Ghana. Minerals (Basel, Switzerland), 2021, 11, 912.	2.0	1